Fully relativistic form factor for Thomson scattering

J. P. Palastro, J. S. Ross, B. Pollock, L. Divol, D. H. Froula, and S. H. Glenzer
Lawrence Livermore National Laboratory, Livermore, California 94551, USA
(Received 22 October 2009; published 24 March 2010)

We derive a fully relativistic form factor for Thomson scattering in unmagnetized plasmas valid to all orders in the normalized electron velocity, $\vec{\beta}=\vec{v}/c$. The form factor is compared to a previously derived expression where the lowest order electron velocity, $\vec{\beta}$, corrections are included [J. Sheffield, *Plasma Scattering of Electromagnetic Radiation* (Academic Press, New York, 1975)]. The $\vec{\beta}$ expansion approach is sufficient for electrostatic waves with small phase velocities such as ion-acoustic waves, but for electron-plasma waves the phase velocities can be near luminal. At high phase velocities, the electron motion acquires relativistic corrections including effective electron mass, relative motion of the electrons and electromagnetic wave, and polarization rotation. These relativistic corrections alter the scattered emission of thermal plasma waves, which manifest as changes in both the peak power and width of the observed Thomson-scattered spectra.

DOI: 10.1103/PhysRevE.81.036411 PACS number(s): 52.27.Ny, 11.80.−m, 52.38.−r, 52.35.Fp

I. INTRODUCTION

Thomson scattering is the process by which an incident light wave accelerates a charged particle, resulting in scattered radiation [1]. For a stationary charge, the scattered radiation has the same frequency as the incident radiation. If the charge is in motion, the scattered radiation has a frequency different from the incident frequency by the Doppler shift: $\omega_s=\omega_i+\vec{k}_i\cdot\vec{v}$, where ω_i is the incident frequency, ω_s the scattered frequency, $\vec{k}_i$ is the wave number of the incident wave, and $\vec{v}$ is the velocity of the charge. When the scattering process occurs in plasma, the excess energy in the scattering process results in a plasma wave, which satisfies the phase matching condition

$$\omega = \omega_s - \omega_i, \tag{1}$$

$$\vec{k}(\omega) = \vec{k}_s(\omega_s) - \vec{k}_i(\omega_i), \tag{2}$$

where ω and $\vec{k}$ are the frequency and wave number of the plasma wave. In terms of the macroscopic plasma behavior, the incident light wave scatters from electrostatic fluctuations (inherent plasma wave spectrum) in the plasma. The connection between single particle and bulk plasma behavior is established through the statistical distribution of velocities and the dielectric response of the bulk plasma.

Thomson scattering in a plasma can be separated into two regimes: noncollective and collective. For optical Thomson scattering, these regimes are delineated by $k\lambda_d$, where $\lambda_d=\sqrt{T_e/4\pi e^2 n_e}$ is the Debye length, T_e is the electron temperature, e is the fundamental unit of charge, and n_e the electron density. In the noncollective regime, $k\lambda_d>1$. The Landau damping of the plasma waves is large, leading to a diffuse fluctuation spectrum. The plasma waves are quasimodes and no natural mode of the plasma is present. In the collective regime, $k\lambda_d<1$, the Thomson spectrum contains four resonances, corresponding to natural modes of the plasma: redshifted and blueshifted features from co- and counterpropagating electron-plasma waves and ion-acoustic waves.

Thomson scattering has proven a critical diagnostic for assessing plasma conditions in laser produced [2–4], tokamak [5–7], and pinch plasmas [8,9]. In each of these systems plasma instabilities develop with growth rates depending sensitively on the plasma conditions. In particular, inertial confinement fusion (ICF) target designs for the National Ignition Facility (NIF) [10] may be susceptible to stimulated Raman scattering [11]. A detailed understanding of the temperature and density of the plasma allows mitigation of Raman scattering and an improvement in ICF margins [10]. The high-density, high-temperature conditions in ICF targets present a new regime for collective Thomson scattering where an understanding of relativistic effects is essential.

In a nonrelativistic development of the Thomson-scattered spectrum, the relative motion between the electron and the incident field only affects the phase of the incident radiation experienced by the electron. The acceleration of the electron is assumed to be independent of velocity (other than the phase), which neglects any modification to the electron trajectory from the Lorentz force and relativity. In noncollective plasmas, these modifications have little consequence on the scattered spectrum unless the electron temperature becomes a sizable fraction of the electron rest energy [12–14]. In collective Thomson scattering, however, the phase velocity of the electron-plasma wave can approach c at moderate or even low electron temperatures. As the Thomson scattering process involves electrons traveling at the phase velocity of the electron-plasma wave, this leads to a situation where relativistic effects can be observed in a plasma traditionally considered nonrelativistic ($T_e \ll m_e c^2$ and $v_{osc}/c \ll 1$) [15].

Relativistic modifications to the Thomson-scattered spectra in both the collective and non-collective regimes have been studied previously [1,12,13,16–18]. Typically, only small relativistic corrections are considered by expanding the scattered electric field of the electron in orders of the normalized electron velocity β and truncating terms higher order than β. In noncollective scattering, the relativistic modifications tend to shift the peak of the scattered radiation to shorter wavelengths with the shift proportional to temperature: charges preferentially emit in the direction of motion. This leads to an increase in the Thomson-scattered power from electrons moving toward the direction of observation and a reduction in power from electrons moving away. Beausang and Prunty have provided a fully relativistic treatment of direct noncollective backscatter [18]. A consideration of only noncollective backscatter geometries limits the usefulness of such a treatment. In collective scattering, relativistic corrections to first order in β, enhance and diminish the blue- and redshifted resonance peaks, respectively. No relativistic treatment of collective scattering in analogy to the Beausang and Prunty publication appears in the literature. Here we present a fully relativistic treatment of Thomson scattering valid to all orders in β, and for all scattering angles perpendicular to the incident polarization for unmagnetized plasmas. The resulting scattered power is generalized for both the collective and noncollective regimes. This generalization allows one to fully explore the extent of relativistic modifications as well as the transition between collective and noncollective scattering.

This paper is organized as follows. In Sec. II, we derive an expression for the fully relativistic scattered power and show that it can be decomposed into a calculation of several integrals. Section III shows correspondence between our result and previous results where relativistic corrections to order β are calculated. Section IV contains an expression for the scattered power valid to an additional order, β^2. In Sec. V, we discuss the physical significance of a fully relativistic treatment. Section VI details our setup for evaluating the fully relativistic form factor numerically. The numerical results for several cases of interest are presented in Sec. VII. Section VIII is the summary and conclusions.

II. RELATIVISTIC FORM FACTOR

A. Scattered power spectrum

We begin by considering an incident plane electric field with an amplitude small enough such that the original trajectory of any electron is only slightly modified (we discuss this further in Appendix A).

$$\vec{E}_i = \vec{E}_{i,0}\cos(\vec{k}_i \cdot \vec{r} - \omega_i t'), \tag{3}$$

where $\vec{k}_i$ and ω_i are the wave number and frequency of the incident wave and t' refers to the retarded time, or time measured in the electron's frame. We will use t to refer to time in the observation frame. For simplicity we choose our observation of the scattered field in the plane perpendicular to the incident electric field as shown in Fig. 1. Defining $\vec{k}_s$ as the wave number of the scattered electromagnetic wave, we can write both $\vec{k}_s \cdot \vec{E}_i = 0$ and $\vec{k}_i \cdot \vec{E}_i = 0$. We also define $\hat{s}$, $\hat{i}$, and $\hat{e}$ as the unit vectors along $\vec{k}_s$, $\vec{k}_i$, and $\vec{E}_i$ respectively, $\beta_s = \hat{s}\cdot\vec{\beta}$, $\beta_i = \hat{i}\cdot\vec{\beta}$, $\beta_E = \hat{e}\cdot\vec{\beta}$, and $c_\theta = \hat{i}\cdot\hat{s}$, which are shown schematically in Fig. 1. If we limit our calculations to an observation distance, R, much larger than both the distance traversed by a charge during the observation time, T, and the sample size, L, only the scattered far field of the electron needs to be considered ($R \gg cT$, $R \gg L$). Under these assumptions we can write the retarded time (electron time), t', in terms of the observation time, t, as follows:

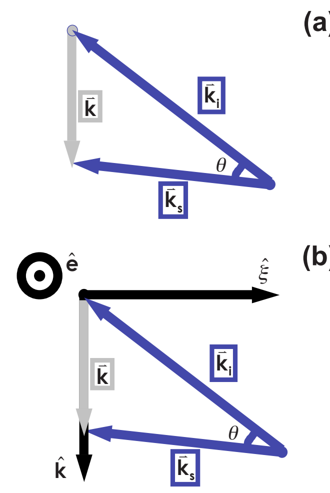

FIG. 1. (Color online) Scattering geometry as defined in text.

$$t' \cong t - \frac{R}{c} + \frac{\hat{s}}{c} \cdot \vec{r}(t), \tag{4}$$

where $\vec{r}(t)$ is the position of the electron in the observation frame. The scattered electric far field due to one electron is then

$$\vec{E}_s(R,t) = \frac{r_e}{R} E_{i,0} \vec{G}(\vec{\beta}) \cos(\vec{k}_i \cdot \vec{r} - \omega_i t'), \tag{5}$$

where r_e is the classical electron radius. The factor $\vec{G}(\vec{\beta})$ is the velocity dependent geometric factor

$$\vec{G}(\vec{\beta}) = \frac{(1-\beta^2)^{1/2}}{(1-\beta_s)^3}[(1-\beta_s)(1-n_i\beta_i)\hat{e} - (n_i c_\theta - \beta_s)\beta_E \hat{s} + n_i(1-\beta_s)\beta_E \hat{i} - (1-n_i c_\theta)\beta_E \vec{\beta}], \tag{6}$$

where $n_i = c|\vec{k}_i|/\omega_i$ is the refractive index of the incident light in the medium, which we return to in Sec. VI D, and $\vec{G}(\vec{\beta})$ is understood to be evaluated in the retarded frame. A proper treatment of $\vec{G}(\vec{\beta})$ is required for a fully relativistic Thomson-scattering form factor, which we present here. Previous treatments have been limited to linearizations of Eq. (6): $\vec{G}(\vec{\beta}) \cong (1+2\beta_s - \beta_i)\hat{e} - c_\theta \beta_E \hat{s} + \beta_E \hat{i}$.

The Klimontovich distribution, which describes precisely the position and velocity of all particles in the plasma, can be expressed as

$$F_e(\vec{r},\vec{v},t') = \sum_j \delta[\vec{r} - \vec{r}_j(t)] \times \delta[\vec{v} - \vec{v}_j(t)]\delta\left[t' - t + \frac{R}{c} - \frac{\hat{s}}{c}\cdot\vec{r}_j(t)\right]. \tag{7}$$

The total scattered electric field can be written as the sum of the scattered electric fields due to each available scatterer. Using the Klimontovich distribution the scattered field is then

$$\vec{E}_s^T(R,t) = \frac{r_e}{R}E_{i,0}\int_V d\vec{r}\int d\vec{v}\vec{G}(\vec{\beta})F_e(\vec{r},\vec{v},t')\cos(\vec{k}_i\cdot\vec{r}-\omega_i t'), \quad (8)$$

where the superscript T refers to total. The time averaged scattered power in a solid angle is then

$$P_s(R,\omega_s) = \frac{cR^2 n_s}{4\pi^2}\lim_{\gamma\to 0}\gamma\int_{\omega_s-\Delta\omega_s/2}^{\omega_s+\Delta\omega_s/2}d\omega_s \times\left|\int_0^\infty dt\vec{E}_s^T(t)e^{-(\gamma+i\omega_s)t}\right|^2, \quad (9)$$

where $n_s=c|\vec{k}_s|/\omega_s$ is the index of refraction for the scattered light. The integration limits represent the fact that the detector collects frequencies within an interval and not at one particular frequency. Because the scattered power is observed at the detector, $n_s=1$.

We seek to evaluate the Laplace transform of $E_s^T(t)$ appearing in Eq. (9), which we can write as

$$L_{\omega_s}[\vec{E}_s^T(t)] = \frac{r_e}{2R}E_{i,0}\int_0^\infty dt'\int_V d\vec{r}\int d\vec{v}\vec{G}'(\vec{\beta})F_e(\vec{r},\vec{v},t') \times[e^{i\vec{k}_+\cdot\vec{r}-i\omega_+t'}+e^{i\vec{k}_-\cdot\vec{r}-i\omega_-t'}], \quad (10)$$

where $L_{\omega_s}[\vec{E}_s^T(t)]=\int dt\vec{E}_s^T(t)e^{-(\gamma+i\omega_s)t}$, we have defined $\vec{G}'(\vec{\beta})\equiv(1-\beta_s)\vec{G}(\vec{\beta})$ and the frequency and wave numbers are defined as follows: $\vec{k}_+=\vec{k}_s+\vec{k}_i$, $\vec{k}_-=\vec{k}_s-\vec{k}_i$, $\omega_+=\omega_s+\omega_i$, and $\omega_-=\omega_s-\omega_i$. Noting that the integrals over time and space are Laplace and Fourier transforms respectively, we find

$$L_{\omega_s}[\vec{E}_s^T(t)] = \frac{r_e}{2R}E_{i,0}\int d\vec{v}\vec{G}'(\vec{\beta})[F_e(\vec{k}_+,\vec{v},\omega_++i\gamma) + F_e(\vec{k}_-,\vec{v},\omega_-+i\gamma)]. \quad (11)$$

The Laplace transforms have been performed assuming a positive scattered frequency, $\omega_s>0$. Allowing ω_s to range over both positive and negative values, we have

$$L_{\pm\omega_s}[\vec{E}_s^T(t)] = \frac{r_e}{2R}E_{i,0}\int d\vec{v}\vec{G}'(\vec{\beta})F_e(\vec{k},\vec{v},\omega+i\gamma), \quad (12)$$

where we have dropped the $\pm$ subscripts, and $\omega=\omega_s-\omega_i$ and $\vec{k}=\vec{k}_s-\vec{k}_i$. Upon substituting Eq. (12) back into Eq. (9) we find the scattered power spectrum to be

$$P_s(R,\omega_s) = \frac{P_i r_e^2}{2\pi a}\lim_{\gamma\to 0}\gamma\left|\int d\vec{v}\vec{G}'(\vec{\beta})F_e(\vec{k},\vec{v},\omega+i\gamma)\right|^2, \quad (13)$$

where $P_i=(cE_{i0}^2/8\pi)a$, and a is the cross-sectional area of the incident beam.

From Eq. (13) When $\vec{G}'(\vec{\beta})$ is approximated as unity we recover the traditional Thomson form factor:

$$S(k,\omega) = \lim_{\gamma\to 0}\gamma\frac{|n_e(k,\omega+i\gamma)|^2}{n_{e0}} \quad (14)$$

by inspection the fully relativistic analog can be written symbolically as

$$S(k,\omega) = \lim_{\gamma\to 0}\frac{\gamma}{n_{e0}}\left|\int d\vec{v}\vec{G}'(\vec{\beta})F_e(\vec{k},\vec{v},\omega+i\gamma)\right|^2. \quad (15)$$

B. Treatment of the Klimontovich distribution function

In order to evaluate $L_{\omega_s}[\vec{E}_s^T(t)]$, we derive an expression for $F_e(\vec{k},\vec{v},\omega)$ that does not require explicit knowledge of the position and velocity of every electron in the system at all times. Expressing the total distributions F_e and F_i as a sum of the average system state $F_{0e}=n_{0e}f_{0e}(\vec{v})$ and $F_{0i}=n_{0,e}f_{0i}(\vec{v})/Z$ (equilibrium distribution) plus a fluctuation contribution, F_{1q}, we have

$$F_e = n_{0e}f_{0e}(\vec{v}) + F_{1e}, \quad (16)$$

$$F_i = Z^{-1}n_{0e}f_{0i}(\vec{v}) + F_{1i}. \quad (17)$$

The equilibrium plasma is taken to be charge neutral such that $\int(f_{0e}-f_{0i})d\vec{v}=0$. The Klimontovich system is composed of the Klimontovich equation

$$\left(\frac{\partial}{\partial t}+\vec{v}\cdot\vec{\nabla}+\frac{q\vec{E}_f}{m_q}\cdot\vec{\nabla}_{\mathrm{p}}\right)F_q=0, \quad (18)$$

where $\vec{\nabla}_{\mathrm{p}}$ is the gradient along the momentum direction and particle-particle correlations have been neglected, and Poisson's equation

$$\vec{\nabla}\cdot\vec{E}_f = 4\pi e\int(ZF_{1i}-F_{1e})d\vec{v}, \quad (19)$$

where $\vec{E}_f$ is the electrostatic field generated by thermal fluctuations. We note that the relativistic Vlasov equation, Eq. (18), is written in terms of the momentum gradient $\vec{\nabla}_{\mathrm{p}}$ and not the velocity gradient $\vec{\nabla}_{\mathrm{v}}$. As a result, the F_q appearing in Eq. (18) is actually the momentum distribution, which can be transformed to the velocity distribution via a Jacobian transformation. From this point on, when an integration is over the coordinates $d\vec{v}$ or $d\vec{p}$ the distributions are understood to be to velocity distributions or momentum distributions, respectively. Furthermore, the operator $\vec{\nabla}_{\mathrm{p}}$ is understood to act on the momentum distribution.

To find F_{1q}, we insert Eqs. (16) and (17) into Eq. (18) and linearize with respect to the fluctuating field amplitude. We find that the fluctuating component of the distribution function can be expressed as follows:

$$F_{1,q}(\vec{k},\vec{v},\omega) = -i\frac{F_{1,q}(\vec{k},\vec{v},t=0)}{\omega-\vec{k}\cdot\vec{v}-i\gamma} - \frac{4\pi q}{mk^2}\frac{\rho_1(\vec{k},\omega)\vec{k}\cdot\vec{\nabla}_{\mathrm{p}}f_{0,q}}{\omega-\vec{k}\cdot\vec{v}-i\gamma}, \quad (20)$$

where $\rho_1(\vec{k},\omega)$ is the spectral fluctuation density

$$\rho_1(\vec{k},\omega) = Zen_{1,i}(\vec{k},\omega) - en_{1,e}(\vec{k},\omega), \tag{21}$$

There are no electromagnetic fluctuations because the electrons are restricted to subluminal phase velocities. In a magnetized plasma, however, slow electromagnetic waves are supported and electrons at subluminal velocities can generate electromagnetic fluctuations.

Before continuing, it useful to note that assuming strait line orbits (a reasonable approximation for weak perturbing fields as shown in Appendix A), the Fourier transform of the Klimontovich distribution can be written as

$$F_e(\vec{k},\vec{v},\omega) = \int d\vec{r}\int dt e^{i(\omega t-\vec{k}\cdot\vec{r})}\sum_j \delta[\vec{r}-\vec{r}_j(t)]\delta[\vec{v}-\vec{v}_j(t)]. \tag{22}$$

or

$$F_e(\vec{k},\vec{v},\omega) = \sum_j e^{-i\vec{k}\cdot\vec{r}_j(0)}\delta[\vec{v}-\vec{v}_j(t)]\delta[\omega-\vec{k}\cdot\vec{v}_j(t)], \tag{23}$$

which we will use in the subsequent algebra.

C. Components of the scattered field spectrum

The Laplace transform, $L_{\omega_s}[\vec{E}_s^T(t)]$, still needs to be evaluated explicitly. We first break the geometric factor, $\vec{G}'$, into four vectors and define H_e, H_s, H_i, and H_p as follows:

$$\vec{H}_e \equiv \hat{e}\int \frac{(1-\beta^2)^{1/2}}{(1-\beta_s)}(1-n_i\beta_i)F_e(\vec{k},\vec{v},\omega)d\vec{v} \tag{24}$$

$$\vec{H}_s \equiv -\hat{s}\int \beta_E\frac{(1-\beta^2)^{1/2}}{(1-\beta_s)^2}(n_ic_\theta-\beta_s)F_e(\vec{k},\vec{v},\omega)d\vec{v} \tag{25}$$

$$\vec{H}_i \equiv \hat{i}\int n_i\beta_E\frac{(1-\beta^2)^{1/2}}{(1-\beta_s)}F_e(\vec{k},\vec{v},\omega)d\vec{v} \tag{26}$$

$$\vec{H}_p \equiv -(1-n_ic_\theta)\int \beta_E\vec{\beta}\frac{(1-\beta^2)^{1/2}}{(1-\beta_s)^2}F_e(\vec{k},\vec{v},\omega)d\vec{v}. \tag{27}$$

In terms of $\vec{H}_e$, $\vec{H}_s$, $\vec{H}_i$, and $\vec{H}_p$, the Laplace transform of the scattered field is simply

$$L_{\omega_s}[\vec{E}_s^T(t)] = \frac{r_e}{2R}E_{i,0}(\vec{H}_e+\vec{H}_s+\vec{H}_i+\vec{H}_p). \tag{28}$$

$\vec{H}_e$, $\vec{H}_s$, and $\vec{H}_i$ are the components of the scattered electric field in the $\hat{e}$, $\hat{s}$, and $\hat{i}$ directions, respectively, for the electrons evolving under the classical Lorentz force of the incident wave, while $\vec{H}_p$ is the additional field component resulting from the polarization rotation of the scattered light from the relativistic motion of the electrons.

We note that when $\theta=\pi$, assuming noncollective behavior: $F_e \to n_{0e}f_{0e}(\vec{v})$, for small density, and taking the distribution function to be symmetric, we recover the scattered field derived by Beausang and Prunty [18] in their relativistic treatment for pure back scattered light in the noncollective regime, namely,

$$L_{\omega_s}[\vec{E}_s^T(t)] = \frac{r_e}{2R}\hat{e}E_{i,0}\int \frac{(1-\beta^2)^{1/2}}{(1-\beta_s)} \times\left[1-\frac{2\beta_E^2}{(1-\beta_s)^2}\right]F_e(\vec{k},\vec{v},\omega)d\vec{v}. \tag{29}$$

In this situation, $\vec{H}_s$, and $\vec{H}_i$ are zero and the second term in square brackets is the modification due to relativistic polarization rotation. Here we are interested in the observed scattered spectra at all available angles perpendicular to the incident polarization.

In Appendix B, we provide a derivation for the following expressions for $\vec{H}_e$, $\vec{H}_s$, $\vec{H}_i$, and $\vec{H}_p$, assuming a symmetric equilibrium distribution function:

$$\vec{H}_e \equiv -\hat{e}i\sum_{j=1}^{N}\frac{(1-\beta^2)^{1/2}(1-n_i\beta_i)}{(1-\beta_s)}\frac{e^{-i\vec{k}\cdot\vec{r}_j(0)}}{\omega-\vec{k}\cdot\vec{v}_j-i\gamma} - \hat{e}\frac{X_e}{e}\rho_1(\vec{k},\omega), \tag{30}$$

$$\vec{H}_s \equiv i\hat{s}\sum_{j=1}^{N}\frac{(1-\beta^2)^{1/2}}{(1-\beta_s)^2}\frac{\beta_E(n_ic_\theta-\beta_s)e^{-i\vec{k}\cdot\vec{r}_j(0)}}{\omega-\vec{k}\cdot\vec{v}_j-i\gamma}, \tag{31}$$

$$\vec{H}_i \equiv -i\hat{i}\sum_{j=1}^{N}\frac{(1-\beta^2)^{1/2}}{(1-\beta_s)}\frac{n_i\beta_E e^{-i\vec{k}\cdot\vec{r}_j(0)}}{\omega-\vec{k}\cdot\vec{v}_j-i\gamma}, \tag{32}$$

$$\vec{H}_p \equiv i(1-n_ic_\theta)\sum_{j=1}^{N}\frac{(1-\beta^2)^{1/2}}{(1-\beta_s)^2}\frac{\beta_E\vec{\beta}e^{-i\vec{k}\cdot\vec{r}_j(0)}}{\omega-\vec{k}\cdot\vec{v}_j-i\gamma}+\frac{\vec{X}_p}{e}\rho_1(\vec{k},\omega), \tag{33}$$

where the spectral fluctuation density is

$$\rho_1(\vec{k},\omega) = -\frac{ie}{\varepsilon}\left[\sum_{j=1}^{N}\frac{e^{-i\vec{k}\cdot\vec{r}_j(0)}}{\omega-\vec{k}\cdot\vec{v}_j-i\gamma}-Z\sum_{l=1}^{N/Z}\frac{e^{-i\vec{k}\cdot\vec{r}_l(0)}}{\omega-\vec{k}\cdot\vec{v}_l-i\gamma}\right], \tag{34}$$

where the sum over l is for ions. The functions X_e and $\vec{X}_p$ can be considered relativistic analogs of the electron susceptibility,

$$X_e \equiv \frac{4\pi e^2}{mk^2}\int \frac{(1-\beta^2)^{1/2}(1-n_i\beta_i)}{(1-\beta_s)}\frac{\vec{k}\cdot\vec{\nabla}_p f_{0,q}}{\omega-\vec{k}\cdot\vec{v}-i\gamma}d\vec{p} \tag{35}$$

$$\vec{X}_p \equiv (1-n_ic_\theta)\frac{4\pi e^2}{mk^2}\int \beta_E\vec{\beta}\frac{(1-\beta^2)^{1/2}}{(1-\beta_s)^2}\frac{\vec{k}\cdot\vec{\nabla}_p f_{0,q}}{\omega-\vec{k}\cdot\vec{v}-i\gamma}d\vec{p}. \tag{36}$$

We note that for small β, $X_e \to \chi_e$, the standard electron susceptibility, while $\vec{X}_p \to 0$.

D. Evaluation of the scattered power

The scattered power, Eq. (15), is proportional to the Poynting flux, which requires an evaluation of $|L_{\omega_s}[\vec{E}_s^T(t)]|^2$. Using our conditions that $\hat{e}\cdot\vec{k}=0$, $\hat{e}\cdot\hat{i}=0$, and $\hat{e}\cdot\hat{s}=0$, there are eight terms that need to be considered in the scattered power: $|\vec{H}_e|^2$, $|\vec{H}_s|^2$, $|\vec{H}_i|^2$, $|\vec{H}_p|^2$, $\vec{H}_e\cdot\vec{H}_p^*$, $\vec{H}_s\cdot\vec{H}_i^*$, $\vec{H}_s\cdot\vec{H}_p^*$, and $\vec{H}_i\cdot\vec{H}_p^*$. The components are considered explicitly in Appendix C. The sum of these components allows for grouping and simplifies the overall expression for $|\vec{H}_e+\vec{H}_s+\vec{H}_i+\vec{H}_p|^2$ into a "few" integrals,

$$\frac{|\vec{H}_e+\vec{H}_s+\vec{H}_i+\vec{H}_p|^2}{N} = \left|\frac{X_e-X_p}{\varepsilon}\right|^2 I_{1e} + \left|\frac{X_e-X_p}{\varepsilon}\right|^2 I_{1i} - 2\,\mathrm{Re}\left[\frac{X_e-X_p}{\varepsilon}\right]\sum_{j=2}^{4} I_j + \sum_{j=5}^{9} I_j, \tag{37}$$

where N is the number of electrons in the scattering volume and I_j are radiation moment integrals, which have the generic form

$$I_j \propto \int d\vec{v}\frac{(1-\beta^2)^{l/2}\beta_e^m\beta_s^n\beta_i^p\beta^q}{(1-\beta_s)^u}\frac{f_e(\vec{\beta})}{(\omega/ck-\hat{k}\cdot\beta)^2+\gamma^2}, \tag{38}$$

where l, m, n, p, q, and u are integers. The specific forms of the integrals are defined in Appendix D. In arriving at Eq. (37), we have used the assumption of a symmetric distribution function to determine that $\vec{X}_p \parallel \hat{e}$ $(X_p=\hat{e}\cdot\vec{X}_p)$. Putting all the components together we arrive at the fully relativistic scattered power for Thomson scattering in unmagnetized plasmas,

$$P_s(\omega_s) = \frac{NP_ir_e^2}{2\pi a}\lim_{\gamma\to 0}\gamma\left\{\left|\frac{X_e-X_p}{\varepsilon}\right|^2 I_{1e} + \left|\frac{X_e-X_p}{\varepsilon}\right|^2 I_{1i} - 2\,\mathrm{Re}\left[\frac{X_e-X_p}{\varepsilon}\right]\sum_{j=2}^{4} I_j + \sum_{j=5}^{9} I_j\right\}. \tag{39}$$

III. CORRESPONDENCE WITH PREVIOUS RESULTS

We now show that our result Eq. (39) reduces to the result given by Sheffield [1] in the nonrelativistic limit, $\beta \ll 1$. We will Taylor expand when necessary, set $n_i=1$, and only retain terms of $O(\vec{\beta})$ in all of our expressions. From the expressions given in Eqs. (D1) thru (D9) we can neglect I_4, I_7, I_8, and I_9. Furthermore, $X_p\sim 0$. At $O(\vec{\beta})$, Eq. (39) simplifies to

$$P_s(\omega_s) = \frac{NP_ir_e^2}{2\pi a}\lim_{\gamma\to 0}\gamma\left\{\left|\frac{X_e}{\varepsilon}\right|^2 I_{1e} + Z\left|\frac{X_e}{\varepsilon}\right|^2 I_{1i} - 2\,\mathrm{Re}\left[\frac{X_e}{\varepsilon}\right]\times[I_2+I_3]+[I_5+I_6]\right\}, \tag{40}$$

where the remaining nonzero expressions are given by

$$X_e \cong \chi_e - \frac{4\pi e^2}{mk^2}\int(\beta_i-\beta_s)\frac{\vec{k}\cdot\vec{\nabla}_v f_{e0}}{\omega-\vec{k}\cdot\vec{v}}d\vec{v}, \tag{41}$$

$$X_e^2 \cong \chi_e^2 - 2\chi_e\frac{4\pi e^2}{mk^2}\int(\beta_i-\beta_s)\frac{\vec{k}\cdot\vec{\nabla}_v f_{e0}}{\omega-\vec{k}\cdot\vec{v}}d\vec{v}, \tag{42}$$

$$I_2+I_3 = \frac{\pi}{\gamma k}\int d\vec{v}(1+\beta_s-\beta_i)h_e, \tag{43}$$

$$I_5+I_6 = \frac{\pi}{\gamma k}\int d\vec{v}(1+2\beta_s-2\beta_i)h_e. \tag{44}$$

Sheffield has demonstrated that the Doppler shifted scattered frequency can be related to the incident frequency via the relation $\omega_s(1-\beta_s)=\omega_i(1-\beta_i)$ [1]. Upon using this relation and the phase matching conditions between the waves we have that $\beta_i-\beta_s=-(\omega/\omega_i)(1-\beta_s)$. Noting that for fixed $\vec{k}$ the assumption that $\beta \ll 1$ is equivalent to $\omega \ll \omega_{s,i}$, we have $\beta_i-\beta_s\cong-(\omega/\omega_i)$, and we reproduce Sheffield's result

$$P_s(\omega_s) = \frac{NP_ir_e^2 n}{2ack}\left(1+2\frac{\omega}{\omega_i}\right)\left[\left|\frac{1+\chi_i}{\varepsilon}\right|^2 f_{e0}^1(\hat{\beta}_k) + Z\left|\frac{\chi_e}{\varepsilon}\right|^2 f_{i0}^1(\hat{\beta}_k)\right], \tag{45}$$

where f_{e0}^1 and f_{i0}^1 are the one-dimensional distribution functions evaluated at $\hat{\beta}_k$ as follows:

$$f_{e0}^1(\hat{\beta}_k) = \frac{e^{-\alpha(1-\hat{\beta}_k^2)^{-1/2}}}{2\alpha^2K_2(\alpha)}\left[1+\left(1+\frac{\alpha}{\sqrt{1-\hat{\beta}_k^2}}\right)^2\right], \tag{46}$$

$$f_{i0}^1(\hat{\beta}_k) = c\left(\frac{M}{2\pi T_i}\right)^{1/2} e^{-Mc^2/2T_i\hat{\beta}_k^2}. \tag{47}$$

For the temperatures considered the nonrelativistic ion distribution is sufficient.

IV. SMALL $\vec{\beta}$ CORRECTION TO SHEFFIELD'S RESULT

For experiments that are only mildly relativistic, it is useful to have a simple expression for the next order corrections to the form factor. Here we maintain terms to order β^2, but we use a nonrelativistic Maxwellian, $\vec{f}_e(\beta)=(2\pi)^{-3/2}(c/v_{Te})^3\exp[-(c\beta/v_{Te})^2/2]$ for evaluation. The error introduced when using the nonrelativistic Maxwellian is generally small at laboratory temperatures $\sim$10 keV as shown in Fig. 2. In addition use of the nonrelativistic Maxwellian greatly simplifies the final expression. By using the nonrelativistic Maxwellian, however, we cannot treat second order thermal corrections, which arise in the deviation between the nonrelativistic and relativistic Maxwellian. We again set $n_i=1$. Using the relation $\beta_i-\beta_s=-(\omega/\omega_i)(1-\beta_s)$, the various components of $P_s(\omega_s)$ can be expressed as follows:

$$I_2+I_3+I_4 = \frac{\pi}{\gamma ck}f_{e0}^1(\hat{\beta}_k)\left(1+\frac{\omega}{\omega_i}-\frac{1}{2}\hat{\beta}_k^2\right), \tag{48}$$

$$I_5+I_6+I_7 = \frac{\pi}{\gamma ck}f_{e0}^1(\hat{\beta}_k)\left[\left(1+\frac{\omega}{\omega_i}\right)^2-\hat{\beta}_k^2\right], \tag{49}$$

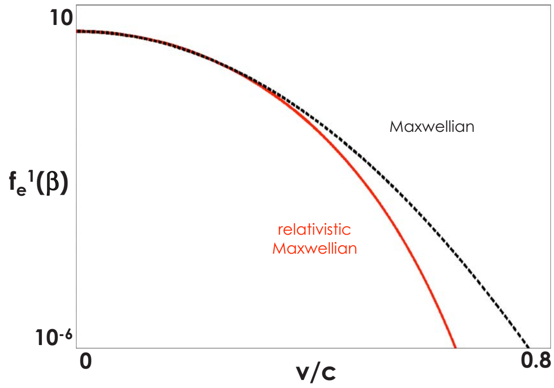

FIG. 2. (Color online) Comparison of 1D velocity distribution functions for $T_e=10$ keV: the nonrelativistic Maxwellian distribution is dotted (black) and the relativistic Maxwellian is solid (red).

$$X_e \cong \left[1+\frac{\omega}{\omega_i}-\frac{1}{2}\hat{\beta}_k^2+(\hat{s}\cdot\hat{k})\left(\frac{v_p}{c}\right)\left(\frac{\omega}{\omega_i}\right)\right]\chi_e-\frac{1}{2}\left(\frac{\omega_p}{\omega}\right)^2\hat{\beta}_k^2, \tag{50}$$

where $\hat{k}$ is the unit vector along $\vec{k}$ and we have used the fact that

$$\frac{4\pi e^2}{mk^2}\int \beta_k^2\frac{\vec{k}\cdot\vec{\nabla}_v f_{e0}}{\omega-\vec{k}\cdot\vec{v}}d\vec{v}=\left(\hat{\beta}_k^2-3\frac{v_{Te}^2}{c^2}\right)\chi_e+\left(\frac{\omega_p}{\omega}\right)^2\hat{\beta}_k^2. \tag{51}$$

We then find that the Thomson-scattered power to order in β^2 can be expressed as $P_s(\omega_s)=P_{e,s}(\omega_s)+P_{i,s}(\omega_s)$, where

$$\begin{aligned}P_{e,s}(\omega_s)=\frac{NP_ir_e^2n}{2cka}f_{e0}^1(\hat{\beta}_k)\Bigg\{&\left[\left(1+\frac{\omega}{\omega_i}\right)^2-\hat{\beta}_k^2+\zeta\left(\frac{\omega}{\omega_i}\right)\hat{\beta}_k\right]\\&\times\left|1-\frac{\chi_e}{\varepsilon}\right|^2+\zeta\left(\frac{\omega}{\omega_i}\right)\hat{\beta}_k\left|\frac{\chi_e}{\varepsilon}\right|^2+\hat{\beta}_k^2\left(\frac{\omega_p}{\omega}\right)^2\\&\times\mathrm{Re}\left[\frac{1+\chi_i}{|\varepsilon|^2}\right]-\frac{1}{2}\hat{\beta}_k^2\Bigg\},\end{aligned} \tag{52}$$

$$\begin{aligned}P_{i,s}(\omega_s)=\frac{NP_ir_e^2n}{2cka}f_{i0}^1(\hat{\beta}_k)\Bigg\{&\left[\left(1+\frac{\omega}{\omega_i}\right)^2-\hat{\beta}_k^2+2\zeta\left(\frac{\omega}{\omega_i}\right)\hat{\beta}_k\right]\\&\times\left|\frac{\chi_e}{\varepsilon}\right|^2-\hat{\beta}_k^2\left(\frac{\omega_p}{\omega}\right)^2\mathrm{Re}\left[\frac{\chi_e}{|\varepsilon|^2}\right]\Bigg\},\end{aligned} \tag{53}$$

and $\zeta=(\hat{k}\cdot\hat{s})$.

V. PHYSICAL INTERPRETATION

The Thomson-scattering form factor describes the total power scattered into electromagnetic waves by a plasma that has been irradiated by an incident electromagnetic wave. For small incident electric field amplitudes (as discussed in Appendix A), the scattered radiation is the sum total of electric dipole fields from electron oscillations in the incident field. For a static dipole the frequency of the emitted radiation is equal to the incident radiation. In a nonzero temperature plasma, each dipole is moving with respect to the propagation axis of the incident radiation. This relative motion results in a velocity dependent scattered frequency or Doppler shift: electrons copropagating with the incident field scatter light at lower frequencies, while electrons counterpropagating scatter light at higher frequencies. Because the dipole oscillators are embedded in the plasma, the scattered frequencies and wave numbers depend on the dielectric properties of the plasma itself.

In the absence of incident radiation, electrons traversing a plasma drive plasma waves producing electrostatic fluctuations in the plasma [19]. The amplitude of the electrostatic fluctuations is determined by how close the frequency of the emitted plasma wave is to the natural mode of the plasma ($\mathrm{Re}[\varepsilon]\cong 0$); emitted waves far from the natural mode frequency are strongly damped and thus have lower amplitudes. In the presence of the incident radiation, the excess photon energy and momentum from the dipole scattering process result in a plasma wave (the excess photon energy is determined by the electron's velocity through the Doppler shift). The plasma is susceptible to the emission of its natural mode, resulting in a scattered radiation spectrum that is weighted by the plasma dielectric susceptibility. The scattered power is thus largest when the difference in frequency between the incident and emitted radiation is close to the plasma frequency.

In the nonrelativistic case, the relative motion between the electron and the incident field only affects the phase of the incident radiation experienced by the electron: each electron oscillates as a stationary dipole with its Doppler modified frequency. In actuality, even for weak incident fields, the motion of the electron in the incident field is quite a bit more complex. The electron motion includes the magnetic field contribution to the Lorentz force and relativistic contributions to the electron motion, including the relativistic rotation of the electromagnetic wave into the electron's frame and changes in the electron's effective mass (in an isotropic thermal plasma irradiated by a plane wave, the electron velocity must be a sizable fraction of c for the magnetic contribution of the Lorentz force to contribute; one can then consider the magnetic contribution to be a relativistic effect). The polarization rotation arises from the scattered power depending on the acceleration and not the force on the electron. When considering the acceleration (time rate of change of velocity) instead of the force, an additional Newtonian "force" arises which resembles the Lorentz transformation of the electric field (the two are identical for $\gamma \gg 1$) [20]. The increase in effective electron mass is straightforward to any one familiar with relativity: the acceleration is not independent of velocity.

In addition to relativistic modifications to the electron motion, the electric field scattered by an electron depends sensitively on the velocity at near luminal speeds. This sensitivity is the direct result of the difference in time between the emission and observation of the scattered photon [20]. If the electron were to move at c, all of the photons scattered from the electron would arrive at the observation point at the same instant, resulting in an unphysically infinite scattered power. At near luminal velocities, the scattered power is enhanced as the photons arrive at the observation point in an effectively shorter duration.

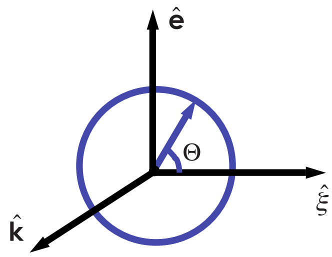

FIG. 3. (Color online) Coordinate system defined for calculation of numerical integrals. The circle lies in the $\hat{\xi}$-ê plane, while $\vec{k}_i$ and $\vec{k}_s$ are in the k̂-$\hat{\xi}$ plane.

In noncollective plasmas, the electron motion has little consequence on the scattered spectrum unless the electron temperature becomes a sizable fraction of the electron rest energy. In collective plasmas, however, the phase velocity of the electron-plasma wave can approach c. The Thomson-scattering process involves electrons traveling at the phase velocity of the electron-plasma wave. This leads to a situation where relativistic effects can be observed in a plasma traditionally considered nonrelativistic ($T_e \ll m_e c^2$ and $v_{osc}/c \ll 1$).

VI. COMPUTATION SETUP

In the previous sections we derived some simple analytic limits for the scattered power. For arbitrary scattering angle and temperature, the scattered power requires numerical evaluation.

A. Reduction of the I_a Integrals

We now focus on reducing the I_a integrals to a form that can be evaluated numerically. We use the singularity to write

$$\int d\vec{\beta} p(\vec{\beta}) \frac{f_{e0}(\vec{\beta})}{(\omega - ck\beta_k)^2 + \gamma^2} = \frac{\pi}{\gamma ck} \int d\vec{\beta} p(\vec{\beta}) f_{e0}(\vec{\beta}) \delta(\beta_k - \hat{\beta}_k), \tag{54}$$

where $p(\vec{\beta})$ represents the various functions proceeding h_e in the I_a integrals and $\hat{\beta}_k = \omega/ck$. With cylindrical coordinates, we can utilize the delta function, and write the h_e integrals as one integral over angle, which can be done analytically, and one angle over "velocity radius" which must be done numerically. We choose one Cartesian velocity axis along $\hat{e}$, the second along $\hat{k}$, and the third to be $\hat{\xi} = \hat{e} \times \hat{k}$ as shown in Fig. 3. Defining $\beta_r = \sqrt{\beta_\xi^2 + \beta_E^2}$, $\beta_\xi = \beta_r \cos \Theta$, and $\beta_E = \beta_r \sin \Theta$, we have

$$\int d\vec{\beta} p(\vec{\beta}) f_{e0}(\vec{\beta}) \delta(\beta_k - \hat{\beta}_k) = \int_0^{2\pi} \int_0^{\sqrt{1-\hat{\beta}_k^2}} p(\beta_r, \hat{\beta}_k, \Theta) \times f_{e0}(\beta_r, \hat{\beta}_k) \beta_r d\beta_r d\Theta. \tag{55}$$

In addition, we define the following angle conversions: $\zeta = (\hat{k} \cdot \hat{s})$, $\eta = (\hat{\xi} \cdot \hat{s})$, $\varpi = (\hat{k} \cdot \hat{i})$, and $\sigma = (\hat{\xi} \cdot \hat{i})$.

Until now we have only assumed that the distribution function is symmetric with respect to β_E. For the duration of this paper, we will focus on the three-dimensional relativistic Maxwellian or Jüttner distribution given as

$$f_{e0}(\vec{\beta}) = \frac{\alpha}{4\pi K_2(\alpha)} \frac{\exp[-\alpha(1-\beta^2)^{-1/2}]}{(1-\beta^2)^{5/2}}, \tag{56}$$

where $\alpha = m_e c^2 / T_e$, $K_2(\alpha)$ is the modified Bessel function of the second kind of order two, and the distribution function is understood to be zero for $\beta \geq 1$. Additional effects such as the effect of inverse Bremsstrahlung on the ion feature and the effect of electron trapping on the electron feature can be considered in future work.

In addition to the integrals in Eqs. (D1)–(D9), we define an additional integral relation $J_n(\alpha, \hat{\beta}_k)$. $J_n(\alpha, \hat{\beta}_k)$ is defined as follows:

$$J_n(\alpha, \hat{\beta}_k) = \frac{\pi}{\gamma ck K_2(\alpha)} \int_0^{\sqrt{1-\hat{\beta}_k^2}} \frac{e^{-\alpha(1-\hat{\beta}_k^2-\beta_r^2)^{-1/2}}}{(1-\hat{\beta}_k^2-\beta_r^2)^{(3+n)/2}} \beta_r d\beta_r, \tag{57}$$

which can be rewritten in terms of derivatives as follows:

$$J_n(\alpha, \hat{\beta}_k) = (-1)^n \frac{\pi}{\gamma ck K_2(\alpha)} \left(\frac{1}{1-\hat{\beta}_k^2} \right)^{1/2} \frac{\partial^n}{\partial \alpha^n} \frac{e^{-\alpha(1-\hat{\beta}_k^2)^{-1/2}}}{\alpha}. \tag{58}$$

We define $J_n(\alpha, \hat{\beta}_k)$ to simplify the forthcoming expressions. An additional factor of $2/\alpha$ has been introduced in the coefficient of f_{e0} as a result of the transition to cylindrical coordinates.

Defining $\psi \equiv (1 - \zeta \hat{\beta}_k)$, each integral involving h_e can be expressed as follows:

$$I_1 = J_2, \tag{59}$$

$$I_2 = \frac{\pi}{\gamma ck K_2(\alpha)} \int_0^{\sqrt{1-\hat{\beta}_k^2}} \times \frac{1}{[\psi^2 - (\eta\beta_r)^2]^{1/2}} \frac{e^{-\alpha(1-\hat{\beta}_k^2-\beta_r^2)^{-1/2}}}{(1-\hat{\beta}_k^2-\beta_r^2)^2} \beta_r d\beta_r, \tag{60}$$

$$I_3 = \varpi \hat{\beta}_k I_2 + \frac{\sigma}{\eta}(\psi I_2 - J_1), \tag{61}$$

$$I_4 = \eta^{-2}(\psi I_2 - J_1), \tag{62}$$

$$I_5 = \frac{\pi\psi}{\gamma ck K_2(\alpha)} \int_0^{\sqrt{1-\hat{\beta}_k^2}} \times \frac{1}{[\psi^2 - (\eta\beta_r)^2]^{3/2}} \frac{e^{-\alpha(1-\hat{\beta}_k^2-\beta_r^2)^{-1/2}}}{(1-\hat{\beta}_k^2-\beta_r^2)^{3/2}} \beta_r d\beta_r, \tag{63}$$

$$I_6 = \varpi\hat{\beta}_k I_5 + \frac{\pi\sigma\eta}{\gamma ck K_2(\alpha)}\int_0^{\sqrt{1-\hat{\beta}_k^2}} \times \frac{1}{[\psi^2-(\eta\beta_r)^2]^{3/2}}\frac{e^{-\alpha(1-\hat{\beta}_k^2-\beta_r^2)^{-1/2}}}{(1-\hat{\beta}_k^2-\beta_r^2)^{3/2}}\beta_r^3 d\beta_r, \quad (64)$$

$$I_7 = \frac{\sigma^2}{\eta^2}J_0 - \left(\varpi^2\hat{\beta}_k^2 + 2\frac{\sigma\varpi}{\eta}\hat{\beta}_k\psi + \frac{\sigma^2}{\eta^2}\psi^2\right)I_5 + 2\left(\varpi\hat{\beta}_k + \frac{\sigma}{\eta}\psi\right)I_6, \quad (65)$$

$$I_8 = -\eta^{-2}J_0 + \frac{\pi\psi\eta^{-2}}{\gamma ck K_2(\alpha)}\int_0^{\sqrt{1-\hat{\beta}_k^2}} \times \frac{1}{[\psi^2-(\eta\beta_r)^2]^{1/2}}\frac{e^{-\alpha(1-\hat{\beta}_k^2-\beta_r^2)^{-1/2}}}{(1-\hat{\beta}_k^2-\beta_r^2)^{3/2}}\beta_r d\beta_r, \quad (66)$$

$$I_9 = \frac{\pi\psi}{2\gamma ck K_2(\alpha)}\int_0^{\sqrt{1-\hat{\beta}_k^2}} \times \frac{1}{[\psi^2-(\eta\beta_r)^2]^{5/2}}\frac{e^{-\alpha(1-\hat{\beta}_k^2-\beta_r^2)^{-1/2}}}{(1-\hat{\beta}_k^2-\beta_r^2)^{1/2}}\beta_r^3 d\beta_r. \quad (67)$$

There are only five unique integrals in the I_a's that must be evaluated numerically I_2, I_5, I_6, I_8, and I_9.

B. Reduction of χ_e, X_e, and X_p

We now reduce our expressions for χ_e, X_e, and X_p in order to simplify the computations required. For χ_e, we start by writing the one-dimensional distribution function with respect to β_k as

$$f_{e0}^1(\beta_k) = \frac{e^{-\alpha(1-\beta_k^2)^{-1/2}}}{2\alpha^2 K_2(\alpha)}\left[1 + \left(1 + \frac{\alpha}{\sqrt{1-\beta_k^2}}\right)^2\right]. \quad (68)$$

Upon differentiating with respect to β_k, we can express χ_e as follows:

$$\chi_e = -\frac{4\pi e^2}{mk}\frac{\alpha}{4\pi c^4 K_2(\alpha)}\int \frac{\beta_k \exp[-\alpha(1-\beta_k^2)^{-1/2}]}{(\omega - \vec{k}\cdot\vec{v})(1-\beta_k^2)^{5/2}}d\beta_k, \quad (69)$$

which requires one numerical integration.

Recall our expressions for X_e and X_p,

$$X_e \equiv \frac{4\pi e^2}{mc^3k^2}\int \frac{(1-\beta^2)^{1/2}(1-n_i\beta_i)}{(1-\beta_s)}\frac{\vec{k}\cdot\vec{\nabla}_p f_{e0}}{\omega - \vec{k}\cdot\vec{v}}d\vec{p}, \quad (70)$$

$$X_p \equiv (1-n_i c_\theta)\frac{4\pi e^2}{mc^3k^2}\int \beta_E^2\frac{(1-\beta^2)^{1/2}}{(1-\beta_s)^2}\frac{\vec{k}\cdot\vec{\nabla}_p f_{e0}}{\omega - \vec{k}\cdot\vec{v}}d\vec{p}. \quad (71)$$

For $\partial f_{e0}(\vec{p})/\partial p_k$ we have

$$\frac{\partial f_{e0}(\vec{p})}{\partial p_k} = -\frac{\alpha}{(1-\beta^2)^{3/2}}\beta_k f_{e0}(\vec{p}), \quad (72)$$

where $f_{e0}(\vec{p})$ is the three-dimensional momentum distribution function. Upon insertion of $\partial f_{e0}(\vec{p})/\partial p_k$, performing a Jacobian transformation from momentum to velocity coordinates, using cylindrical coordinates, and integrating over Θ and β_r provides the following:

$$X_e = \frac{2\pi e^2\alpha}{mc^3k^2K_2(\alpha)}\frac{\sigma}{\eta}\int_{-1}^{1}\frac{g_A(\beta_k)Q(\alpha,\beta_k) + P(\alpha,\beta_k)}{(\hat{\beta}_k - \beta_k)}d\beta_k, \quad (73)$$

$$X_p = (1-n_i c_\theta)\frac{2\pi e^2\alpha\eta^{-2}}{mc^3k^2K_2(\alpha)} \times \int_{-1}^{1}\frac{g_D(\beta_k)Q(\alpha,\beta_k) - P(\alpha,\beta_k)}{(\hat{\beta}_k - \beta_k)}d\beta_k, \quad (74)$$

where we have again used $\beta_r = \sqrt{\beta_\xi^2 + \beta_E^2}$, $\beta_\xi = \beta_r \cos\Theta$, and $\beta_E = \beta_r \sin\Theta$.

Q, P, g_A, and g_D were defined for numerical purposes and are given as follows:

$$Q(\alpha,\beta_k) = -\alpha\beta_k \times \int_0^{\sqrt{1-\beta_k^2}}\frac{\beta_r e^{-\alpha(1-\beta^2)^{-1/2}}}{[(1-\zeta\beta_k)^2 - (\eta\beta_r)^2]^{1/2}(1-\beta^2)^{7/2}}d\beta_r, \quad (75)$$

$$P(\alpha,\beta_k) = -\alpha\beta_k\int_0^{\sqrt{1-\beta_k^2}}\frac{\beta_r e^{-\alpha(1-\beta^2)^{-1/2}}}{(1-\beta^2)^{7/2}}d\beta_r, \quad (76)$$

$g_A = (\eta/\sigma - n_i) - n_i(\eta\varpi/\sigma - \zeta)\beta_k$, and $g_D = 1 - \zeta\beta_k$. We can then compute the fully relativistic form factor with two look up tables and eight one-dimensional numerical integrals, three of which require a treatment of the singularity at $\beta_k = \hat{\beta}_k$.

C. Numerical Integration of χ_e, X_e, and X_p

The numerical integrals for χ_e, X_e, and X_p [Eqs. (69), (73), and (74), respectively] all include singularities (simple poles) which require careful evaluation. Symbolically, the singular integrals can be evaluated using Plemlj's formula

$$\lim_{\nu\to 0}\frac{1}{\hat{\beta}_k \pm i\nu - \beta_k} = PV\frac{1}{\hat{\beta}_k - \beta_k} \mp i\pi\delta(\hat{\beta}_k - \beta_k), \quad (77)$$

where PV is principle value abbreviated and the formula is defined under an integral. Here we outline our numerical equivalent to Plemelj's formula [21].

We start by writing the general form of the integral in three parts as follows:

$$\int_{-1}^{1}\frac{h(\beta_k)}{\hat{\beta}_k-\beta_k}d\beta_k=\left[\int_{-1}^{\hat{\beta}_k-\varphi}+\int_{\hat{\beta}_k+\varphi}^{1}+\int_{\hat{\beta}_k-\varphi}^{\hat{\beta}_k+\varphi}\right]\frac{h(\beta_k)}{\hat{\beta}_k-\beta_k}d\beta_k. \tag{78}$$

To calculate the first two integrals numerically we must choose a nonzero value for phi. Choosing $\varphi=\ell(1-|\hat{\beta}_k|)$, where $0<\ell\ll 1$, and defining the numerical step size as $\Delta\beta_k=w\varphi$, where $0<w\ll 1$, allows for an increase in numerical grid resolution when the phase velocity approaches c ($\Delta\beta_k\to 0$ as $|\hat{\beta}_k|\to 1$). This method also minimizes the error in the cancellations that occur in the first two integrals near the singularity (the integral is odd around the singularity). To further minimize the cancellation error, we define symmetric arrays for evaluating the first two integrals as follows: $\beta_{k,-}=\hat{\beta}_k-\varphi-(p-1)\Delta\beta_k$ and $\beta_{k,+}=\hat{\beta}_k+\varphi+(m-1)\Delta\beta_k$, where $\beta_{k,-}>-1$ and $\beta_{k,+}<1$ are the arrays for the upper and lower integrals respectively, and m and p are integers. With these arrays defined the upper and lower integrals can be performed using standard numerical integration. For the pole contribution we linearize $h(\beta_k)$ around $\hat{\beta}_k$ and integrate to find

$$\int_{\hat{\beta}_k-\varphi}^{\hat{\beta}_k+\varphi}\frac{h(\beta_k)}{\hat{\beta}_k-\beta_k}d\beta_k=-i\pi h(\hat{\beta}_k)+2\varphi\frac{dh(\hat{\beta}_k)}{d\beta_k}. \tag{79}$$

The first term represents the delta function of Plemelj's formula, while the second is the correction due to the finite value of phi required for numerical evaluation. The derivative of $h(\beta_k)$ can be found using standard numerical differentiation.

D. Index of refraction of incident light

The dispersion relation for a light wave propagating in a plasma can be expressed as follows:

$$\frac{\omega_i^2}{c^2}-k_i^2+\omega_i\frac{\omega_{p,e}^2}{c}\int\frac{\beta_e}{1-\beta^2}\left[\frac{\hat{e}-\vec{\beta}\beta_e}{\omega_i-ck_i\beta_i}\right]\cdot\vec{\nabla}_v f_{0,e}d\vec{v}=0, \tag{80}$$

where we have assumed that $f_{0,e}$ is a symmetric function of velocity. The index of refraction is then

$$n_i^2=1-\frac{\alpha^2}{4K_2(\alpha)}\frac{\omega_{p,e}^2}{\omega_i ck_i}\int\frac{\beta_r^3}{[1-\beta_r^2-\beta_i^2]^{3/2}}\times\left(\frac{1}{\hat{\beta}_i-\beta_i}\right)e^{-\alpha(1-\beta_r^2-\beta_i^2)^{-1/2}}d\beta_r d\beta_i. \tag{81}$$

Equation can be solved with an iterative method with the solution used in the phase matching of the waves. The scattered wave number is found in the same manner.

VII. COMPUTATIONAL RESULTS

To examine how the relativistic and nonrelativistic scattered power spectra differ, we use the elements of Secs. II and III to evaluate the power spectrum to all orders in β. We will focus on ICF-like plasma conditions, which tend to be more collective in nature, $k\lambda_d<1$, but can become more noncollective, $k\lambda_d>1$, at higher temperatures. We note that our derived spectra do not include the effects of magnetic fields, but we can examine to what extent additional relativistic effects play a roll. The results will thus be limited to plasma parameters for which $kr_L>1$, where r_L is the thermal Larmor radius given by mv_{Te}/eB.

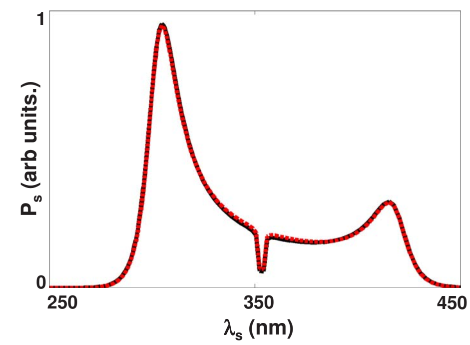

FIG. 4. (Color online) Comparison of our computed scattered spectrum to the analytic expression given in Eq. (43). The computed line is in red (dashed), the analytic result in black (solid).

To demonstrate that our computations are correct, we consider the nonrelativistic limit of our calculation. The nonrelativistic limit requires scattering from low phase velocity plasma waves (small n/n_c) and at low temperatures (small T_e/m_ec^2). We consider scattering of a 351 nm incident beam at 90° in a plasma with a temperature of 1 keV and $n/n_c=0.011$. Figure 4 shows a comparison of our computation with Eq. (45) given by Sheffield as one would see on a standard camera (plotted versus scattered wavelength and using $\Delta\omega_s=2\pi c\Delta\lambda_s/\lambda_s^2$). The dotted line is the relativistic and solid line is the spectrum given by Eq. (39). The ion feature has been masked for clarity. The agreement is apparent.

At higher densities and temperatures the deviations of the first order relativistic corrections from the fully relativistic form factor become increasingly pronounced. Figure 5 shows comparisons of the scattered power from both treatments on a log scale as a function of frequency for T_e

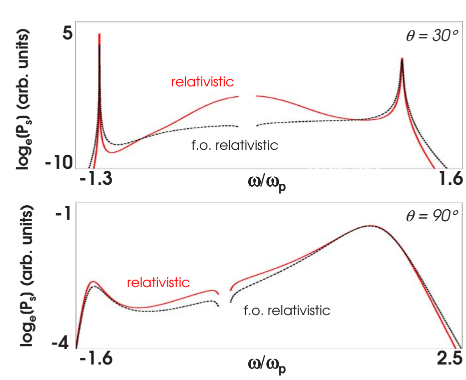

FIG. 5. (Color online) Natural logarithm of the scattered power as a function of plasma wave frequency for $T_e=5$ keV and $n_e/n_c=0.05$. The top plot shows the form factor comparison at a scattering angle 30° and the bottom at 90°. The relativistic is in red (solid); the first order relativistic in black (dashed).

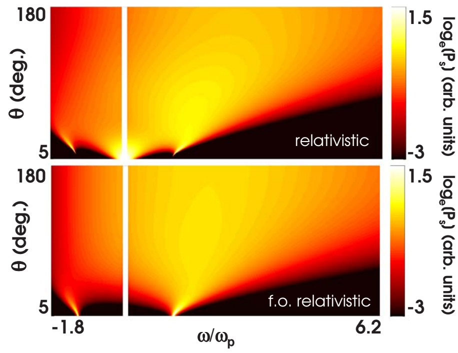

FIG. 6. (Color online) Natural logarithm of the scattered power as a function of scattering angle, θ, and plasma wave frequency for T_e=25 keV and n_e/n_c=0.05. The top plot shows our fully relativistic calculation and the bottom the nonrelativistic form factor with the first-order relativistic correction.

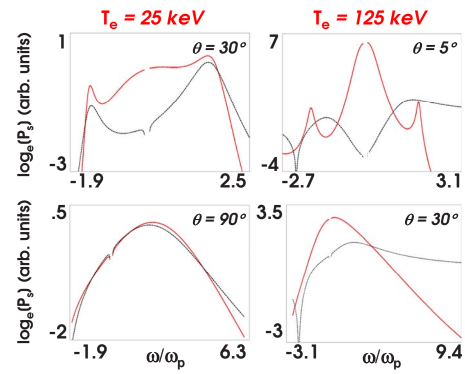

FIG. 7. (Color online) Natural logarithm of the scattered power as a function of plasma wave frequency at n_e/n_c=0.05 for T_e=25 keV and T_e=125 keV on the left and right, respectively. The top and bottom T_e=25 keV plots are at scattering angles of 30° and 90°, respectively, while the T_e=125 keV are at angles of 5° and 30°. The relativistic is in red (solid) while the first order relativistic correction is in black (dashed).

=5 keV and n_e=0.05 n_c. At 30°, the redshifted peak has a higher amplitude and a slight frequency shift in the fully relativistic treatment. A more obvious difference is the enhancement of the scattered power at small frequencies. The enhancement results from the integrals I_6 and I_7 which involve integrals of β_i, and does not occur when approximated through linearization (as in previous treatments). From a physical standpoint, even though the electrons involved in the scattering process have a low velocity in the propagation direction of the plasma wave, they can still have relativistic velocities in the perpendicular direction. This perpendicular relativistic motion is completely missed in the first-order treatment. At 90° this enhancement disappears and the two form factors are similar. At 30°, $\hat{i}$ and $\hat{k}$ are nearly perpendicular and thus β_i can reach relativistic levels, while at 90° $\hat{i}$ and $\hat{k}$ are nearly antiparallel and the magnitude of β_i must be closer to the phase velocity of the plasma wave, which is much smaller than c at the frequencies of the enhancement. This disparity in the range of valid β_i causes the emergence and disappearance of the enhancement and is not observed in the standard form factor as β_i can range from $-\infty$ to ∞.

Figure 6 shows a comparison of the log of the scattered power resulting from the relativistic treatment (top) and the first-order (bottom) correction as a function of frequency and scattering angle at T_e=25 keV and n_e/n_c=0.05. The low frequency enhancement is apparent in the relativistic plot. Other than the bulk changes in the collective regime (large angles), the fully relativistic peaks are narrower (less damped) than the first order relativistic. The reduced damping is in part due to the reduction in the number of electrons available to take energy from the plasma wave at higher velocities which can be seen in a comparison of relativistic Maxwellian and nonrelativistic Maxwellian as seen in Fig. 2.

In Fig. 7 the log of the scattered power is plotted as a function of frequency for four different cases: T_e=25 keV for θ=30° and 90°, and T_e=125 keV for θ=5° and 30°. The relativistic is plotted in red (solid) and the first-order relativistic in black (dashed). For both temperatures the spectrum becomes more noncollective as the angle increases, but the transition to noncollective occurs at a much smaller angle at T_e=125 keV. This is direct result of the temperature dependence $k\lambda_d \propto \sqrt{T_e}$. At higher $k\lambda_d$ the Landau damping eliminates the collective behavior of the plasma. For T_e=125 keV and θ=5° the first-order relativistic form factor becomes insufficient for capturing the natural response of the plasma, which is seen in the absence of the low frequency enhancement and the width and amplitude of the collective peaks.

A temperature scaling comparison of the log of the scattered power at θ=45° and n_e/n_c=0.20 is depicted in Fig. 8. The cutoff at ω=$-1.2\omega_p$ marks where the scattered frequency becomes smaller than the plasma frequency. The first-order relativistic becomes negative at $\omega < -\omega_i/2$ as seen in Eq. (45). Line plot comparisons of two different densities and temperatures at θ=45° are shown in Fig. 5. The top plot has n_e/n_c=0.12 and T_e=10 keV while the bottom plot has n_e/n_c=0.20 and T_e=20 keV. The difference between the fully relativistic and first order relativistic is substantial in both the width of the blueshifted peak and in the occurrence of the low frequency enhancement (Fig. 9).

VIII. SUMMARY AND CONCLUSIONS

We have derived a fully relativistic form factor for Thomson scattering in the weak pump limit. For scattering from electron-plasma waves a fully relativistic treatment is necessary as the phase velocity of the waves can be near luminal. The form factor greatly improves on previous treatments, which treated relativistic effects by expansions in the normalized electron velocity β. The derivation extended the treatment of Sheffield [1] by treating the scattered electric field from an accelerated charge in a nonperturbative manner. The resulting expression was written as a sum of integral expressions, which require knowledge of the one-dimensional electron distribution function for evaluation. The form factor makes no assumption about the collective or noncollective nature of the scattering and thus can be used to analyze both cases and transitions between them. In addition, our fully relativistic treatment is valid for any scattering

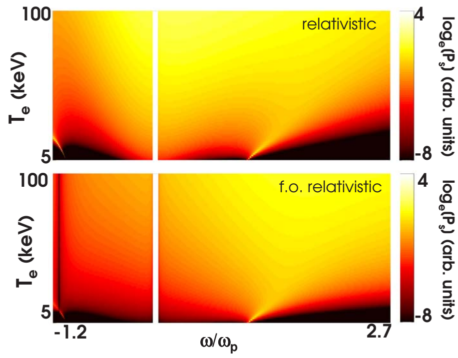

FIG. 8. (Color online) Natural logarithm of the scattered power as a function of electron temperature, and plasma wave frequency for $\theta=45°$ and $n_e/n_c=0.20$. The top plot shows our fully relativistic calculation and the bottom the nonrelativistic form factor with the first order relativistic correction.

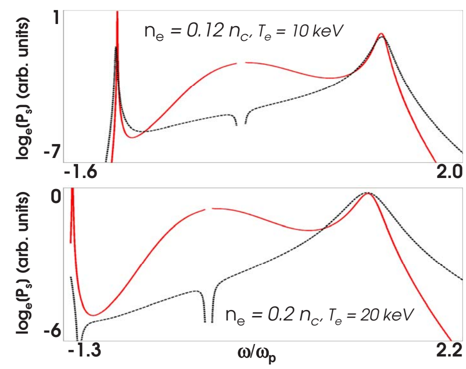

FIG. 9. (Color online) Natural logarithm of the scattered power as a function of plasma wave frequency at a scattering angle of $\theta=45°$. The top plot shows the form factor comparison at a $T_e=10$ keV and $n_e/n_c=0.12$ while the bottom plot shows $T_e=20$ keV and $n_e/n_c=0.2$. The relativistic is in red (solid) while the first order relativistic correction is in black (dashed).

angle such that the scattering plane is perpendicular to the incident electric field vector.

Two of the major results of the fully relativistic treatment are the enhancement in low frequency signal and the bulk changes in the scattered power including spectral shape, width, and amplitude. The low frequency enhancement results from electrons contributing to the wave scattering having relativistic velocities perpendicular to the phase velocity even when the phase velocity is much smaller than c. A proper Thomson-scattered spectrum is important to precisely determine the bulk plasma conditions and to ensure an appropriate noise source for the growth of stimulated Raman scattering.

ACKNOWLEDGMENTS

The authors would like to thank E. A. Williams and J. Sheffield for fruitful discussions. Prepared by LLNL under Contract No. DE-AC52-07NA27344; Tracking Numbers ERD-08-017 and 08-LW-070.

APPENDIX A: TRAJECTORY MODIFICATION FROM THE INCIDENT FIELD

For a condition on the change in electron trajectory due to the presence of the electromagnetic field we perform an expansion of the electron motion as follows:

$$\vec{s}(t) = \vec{s}_0 + \vec{v}_0 t + \delta\vec{s}(t), \tag{A1}$$

$$\gamma(t) = \gamma_0 + \delta\gamma(t), \tag{A2}$$

where $\vec{s}=(x,y,z)$, γ is the relativistic factor, $\gamma_0=(1-v_0^2/c^2)^{1/2}$, and $\delta\vec{s}(t)$ and $\delta\gamma(t)$ represent the change in the trajectory due to the electromagnetic field. For small changes in the trajectory one can show that $\delta\gamma \cong \gamma_0^3(\vec{v}_0\cdot\delta\vec{s})/c^2$. The force equations for our perturbed quantities are then

$$\delta\ddot{x} = \left[1+\gamma_0^2\left(\frac{v_0}{c}\right)^2\right]^{-1}\frac{qE_{i,0}}{\gamma_0 m_e c}\left[1-\left(\frac{v_{z,0}}{c}\right)\right]\cos[(\omega_i - k_i v_{z0})t], \tag{A3}$$

$$\delta\ddot{y} = \left[1+\gamma_0^2\left(\frac{v_0}{c}\right)^2\right]^{-1}\frac{qE_{i,0}}{\gamma_0 m_e c}\left[1+\left(\frac{v_{z,0}}{c}\right)\right]\cos[(\omega_i - k_i v_{z0})t], \tag{A4}$$

$$\delta\ddot{z} = \left[1+\gamma_0^2\left(\frac{v_0}{c}\right)^2\right]^{-1}\frac{qE_{i,0}}{\gamma_0 m_e c}\left(\frac{v_{x,0}}{c}\right)\cos[(\omega_i - k_i v_{z0})t], \tag{A5}$$

where we have approximated $c|k_i|/\omega_i$ as unity. The maximum excursion for an electron in the electromagnetic field can be approximated as

$$\delta s_{\max} \cong \frac{2}{k_i}\left[1+\gamma_0^2\left(\frac{v_0}{c}\right)^2\right]^{-1}\left(\frac{v_{osc}}{c}\right)\left(\frac{c}{c-v_{z0}}\right)^2, \tag{A6}$$

where $v_{osc}=k_i^{-1}(qE_{i,0}/\gamma_0 m_e c)$ is the relativistic oscillation velocity. We compare Eq. (A6) with the excursion of an electron unperturbed by the laser field over one laser period, namely v_0/ω_i. Taking the ratio, we find the condition for small perturbed excursions is simply,

$$2\left[1+\gamma_0^2\left(\frac{v_0}{c}\right)^2\right]^{-1}\left(\frac{v_{osc}}{v_0}\right)\left(\frac{c}{c-v_{z0}}\right)^2 \ll 1. \tag{A7}$$

Assuming a thermal plasma, Eq. (A7) simplifies to $v_{osc} \ll v_{T,e}$ for nonrelativistic electrons, while for relativistic electrons we have $8\gamma_0^2 v_{osc} \ll c$.

APPENDIX B: EXPRESSIONS FOR $\vec{H}_e$, $\vec{H}_s$, $\vec{H}_i$, and $\vec{H}_p$

Here we will focus on evaluating $\vec{H}_e$ and note that evaluation of $\vec{H}_s$, $\vec{H}_i$, and $\vec{H}_p$ follow the same general procedure. Inserting Eq. (18) into $\vec{H}_e$ provides the following

$$\vec{H}_e \equiv -\hat{e}\int \frac{(1-\beta^2)^{1/2}}{(1-\beta_s)}(1-n_i\beta_i)\left[i\frac{F_{1,q}(\vec{k},\vec{v},t=0)}{\omega-\vec{k}\cdot\vec{v}-i\gamma}d\vec{v} + \frac{4\pi q}{mk^2}\frac{\rho_1(\vec{k},\omega)\vec{k}\cdot\vec{\nabla}_{\mathrm{p}}f_{0,q}}{\omega-\vec{k}\cdot\vec{v}-i\gamma}d\vec{p}\right] \tag{B1}$$

where we have dropped the contribution of F_{0q} to F_q; this term limits to zero as $\gamma \to 0$ and represents only a transient response of the plasma. The second integral in Eq. (B1) is over $d\vec{p}$ and cannot be transformed to a velocity integral until the operator $\vec{\nabla}_{\mathrm{p}}$ is applied. Rewriting Eq. (B1), we have the following:

$$\vec{H}_e \equiv -i\hat{e}\sum_{j=1}^{N}\frac{(1-\beta^2)^{1/2}(1-n_i\beta_i)}{(1-\beta_s)}\frac{e^{-i\vec{k}\cdot\vec{r}_j(0)}}{\omega-\vec{k}\cdot\vec{v}_j-i\gamma} - \hat{e}\frac{X_e}{e}\rho_1(\vec{k},\omega) \tag{B2}$$

where we have defined

$$X_e \equiv \frac{4\pi e^2}{mk^2}\int \frac{(1-\beta^2)^{1/2}(1-n_i\beta_i)}{(1-\beta_s)}\frac{\vec{k}\cdot\vec{\nabla}_{\mathrm{p}}f_{0,q}}{\omega-\vec{k}\cdot\vec{v}-i\gamma}d\vec{p}. \tag{B3}$$

Similarly, we have

$$\vec{H}_s \equiv i\hat{s}\sum_{j=1}^{N}\beta_E\frac{(1-\beta^2)^{1/2}}{(1-\beta_s)^2}(n_ic_\theta-\beta_s)\frac{e^{-i\vec{k}\cdot\vec{r}_j(0)}}{\omega-\vec{k}\cdot\vec{v}_j-i\gamma} + \hat{s}\frac{X_s}{e}\rho_1(\vec{k},\omega), \tag{B4}$$

$$X_s \equiv \frac{4\pi e^2}{mk^2}\int \beta_E\frac{(1-\beta^2)^{1/2}}{(1-\beta_s)^2}(n_ic_\theta-\beta_s)\frac{\vec{k}\cdot\vec{\nabla}_{\mathrm{p}}f_{0,q}}{\omega-\vec{k}\cdot\vec{v}-i\gamma}d\vec{p}, \tag{B5}$$

$$\vec{H}_i \equiv -i\hat{i}\sum_{j=1}^{N}n_i\beta_E\frac{(1-\beta^2)^{1/2}}{(1-\beta_s)}\frac{e^{-i\vec{k}\cdot\vec{r}_j(0)}}{\omega-\vec{k}\cdot\vec{v}_j-i\gamma} - \hat{i}\frac{X_i}{e}\rho_1(\vec{k},\omega), \tag{B6}$$

$$X_i \equiv \frac{4\pi e^2}{mk^2}\int n_i\beta_E\frac{(1-\beta^2)^{1/2}}{(1-\beta_s)}\frac{\vec{k}\cdot\vec{\nabla}_{\mathrm{p}}f_{0,q}}{\omega-\vec{k}\cdot\vec{v}-i\gamma}d\vec{p} \tag{B7}$$

$$\vec{H}_p \equiv i(1-n_ic_\theta)\sum_{j=1}^{N}\beta_E\vec{\beta}\frac{(1-\beta^2)^{1/2}}{(1-\beta_s)^2}\frac{e^{-i\vec{k}\cdot\vec{r}_j(0)}}{\omega-\vec{k}\cdot\vec{v}_j-i\gamma} + \frac{\vec{X}_p}{e}\rho_1(\vec{k},\omega) \tag{B8}$$

$$X_p \equiv (1-n_ic_\theta)\frac{4\pi e^2}{mk^2}\int \beta_E\vec{\beta}\frac{(1-\beta^2)^{1/2}}{(1-\beta_s)^2}\frac{\vec{k}\cdot\vec{\nabla}_{\mathrm{p}}f_{0,q}}{\omega-\vec{k}\cdot\vec{v}-i\gamma}d\vec{p}. \tag{B9}$$

Similar expressions are obtained for the ions with $\rho_1(\vec{k},\omega) \to -\rho_1(\vec{k},\omega)$. For simplicity we will only consider distribution functions with symmetry in velocity space, which implies $X_s = X_i = 0$. The resulting set of equations are given by Eqs. (30)–(36).

APPENDIX C: EXPRESSIONS FOR COMPONENTS OF THE POYNTING FLUX

As in Appendix B, we consider one term in detail, $|\vec{H}_e|^2$, and note that the derivation of other terms follows the same general procedure.

$$\begin{aligned}
|\vec{H}_e|^2 = {} & \sum_{j=1}^{N}\frac{(1-\beta^2)^{1/2}(1-n_i\beta_i)}{(1-\beta_s)}\frac{e^{-i\vec{k}\cdot\vec{r}_j(0)}}{\omega-\vec{k}\cdot\vec{v}_j-i\gamma} \\
& \times\sum_{n=1}^{N}\frac{(1-\beta^2)^{1/2}(1-n_i\beta_i)}{(1-\beta_s)}\frac{e^{i\vec{k}\cdot\vec{r}_n(0)}}{\omega-\vec{k}\cdot\vec{v}_n+i\gamma} \\
& + \left|\frac{X_e}{\varepsilon}\right|^2\left|\sum_{j=1}^{N}\frac{e^{-i\vec{k}\cdot\vec{r}_j(0)}}{\omega-\vec{k}\cdot\vec{v}_j-i\gamma} - Z\sum_{l=1}^{N/Z}\frac{e^{-i\vec{k}\cdot\vec{r}_l(0)}}{\omega-\vec{k}\cdot\vec{v}_l-i\gamma}\right|^2 \\
& - \frac{X_e}{\varepsilon}\left(\sum_{j=1}^{N}\frac{e^{-i\vec{k}\cdot\vec{r}_j(0)}}{\omega-\vec{k}\cdot\vec{v}_j-i\gamma} - Z\sum_{l=1}^{N/Z}\frac{e^{-i\vec{k}\cdot\vec{r}_l(0)}}{\omega-\vec{k}\cdot\vec{v}_l-i\gamma}\right) \\
& \times\sum_{n=1}^{N}\frac{(1-\beta^2)^{1/2}(1-n_i\beta_i)}{(1-\beta_s)}\frac{e^{i\vec{k}\cdot\vec{r}_n(0)}}{\omega-\vec{k}\cdot\vec{v}_n+i\gamma} \\
& - \frac{X_e^*}{\varepsilon^*}\left(\sum_{j=1}^{N}\frac{e^{i\vec{k}\cdot\vec{r}_j(0)}}{\omega-\vec{k}\cdot\vec{v}_j+i\gamma} - Z\sum_{l=1}^{N/Z}\frac{e^{\vec{k}\cdot\vec{r}_l(0)}}{\omega-\vec{k}\cdot\vec{v}_l+i\gamma}\right) \\
& \times\sum_{n=1}^{N}\frac{(1-\beta^2)^{1/2}(1-n_i\beta_i)}{(1-\beta_s)}\frac{e^{-i\vec{k}\cdot\vec{r}_n(0)}}{\omega-\vec{k}\cdot\vec{v}_n-i\gamma}
\end{aligned} \tag{C1}$$

We say that the electrons and ions are spatially uncorrelated, which allows us to drop cross terms in the summations. Defining

$$h_q(\vec{k},\vec{v},\omega) \equiv \frac{f_{q0}(\vec{v})}{(\omega-\vec{k}\cdot\vec{v})^2+\gamma^2}, \tag{C2}$$

we find

$$\frac{|\vec{H}_e|^2}{N} = \int d\vec{v}\left|\frac{(1-\beta^2)^{1/2}(1-n_i\beta_i)}{(1-\beta_s)} - \frac{X_e}{\varepsilon}\right|^2 h_e + \left|\frac{X_e}{\varepsilon}\right|^2\int d\vec{v}h_i. \tag{C3}$$

Similarly we have for $|\vec{H}_s|^2$, $|\vec{H}_i|^2$, and $|\vec{H}_p|^2$

$$\frac{|\vec{H}_s|^2}{N} = \int d\vec{v}\frac{(1-\beta^2)\beta_E^2}{(1-\beta_s)^4}(n_ic_\theta-\beta_s)^2 h_e \tag{C4}$$

$$\frac{|\vec{H}_i|^2}{N} = n_i^2 \int d\vec{v} \frac{(1-\beta^2)\beta_E^2}{(1-\beta_s)^2} h_e \tag{C5}$$

$$\frac{|\vec{H}_p|_2}{N} = \int d\vec{v} \left| (1-n_i c_\theta) \frac{(1-\beta^2)^{1/2} \vec{\beta}\beta_E}{(1-\beta_s)^2} - \frac{\vec{X}_p}{\varepsilon} \right|^2 h_e + \left| \frac{X_p}{\varepsilon} \right|^2 \int d\vec{v} h_i. \tag{C6}$$

For the cross terms, we use the fact that $\hat{s}\cdot\vec{X}_D^*=0$ and $\hat{i}\cdot\vec{X}_D^*=0$ to find the following:

$$\frac{\vec{H}_s \cdot \vec{H}_i^*}{N} = -n_i c_\theta \int d\vec{v} (n_i c_\theta - \beta_s) \frac{(1-\beta^2)\beta_E^2}{(1-\beta_s)^3} h_e, \tag{C7}$$

$$\frac{\vec{H}_e \cdot \vec{H}_p^*}{N} = -\int d\vec{v} \left[\frac{X_e}{\varepsilon} - \frac{(1-\beta^2)^{1/2}(1-n_i\beta_i)}{(1-\beta_s)} \right] \left[\frac{(\hat{e}\cdot X_p^*)}{\varepsilon^*} - (1-n_i c_\theta) \frac{(1-\beta^2)^{1/2}\beta_E^2}{(1-\beta_s)^2} \right] h_e - \frac{X_e(\hat{e}\cdot X_p^*)}{|\varepsilon|^2} \int d\vec{v} h_i \tag{C8}$$

$$\frac{\vec{H}_s \cdot \vec{H}_p^*}{N} = (1-n_i c_\theta) \int d\vec{v} (n_i c_\theta - \beta_s) \frac{(1-\beta^2)\beta_E^2 \beta_s}{(1-\beta_s)^4} h_e \tag{C9}$$

$$\frac{\vec{H}_i \cdot \vec{H}_p^*}{N} = -n_i(1-n_i c_\theta) \int d\vec{v} \frac{(1-\beta^2)\beta_E^2 \beta_i}{(1-\beta_s)^3} h_e. \tag{C10}$$

APPENDIX D: DEFINITIONS OF I_j

In evaluating the Poynting flux, we defined the following radiation integrals,

$$I_{1q} = \int d\vec{v} h_q, \tag{D1}$$

$$I_2 = \int d\vec{v} \frac{(1-\beta^2)^{1/2}}{(1-\beta_s)} h_e, \tag{D2}$$

$$I_3 = -n_i \int d\vec{v} \frac{(1-\beta^2)^{1/2}\beta_i}{(1-\beta_s)} h_e, \tag{D3}$$

$$I_4 = -(1-n_i c_\theta) \int d\vec{v} \frac{(1-\beta^2)^{1/2}\beta_E^2}{(1-\beta_s)^2} h_e, \tag{D4}$$

$$I_5 = \int d\vec{v} \frac{(1-\beta^2)}{(1-\beta_s)^2} h_e, \tag{D5}$$

$$I_6 = -2n_i \int d\vec{v} \frac{(1-\beta^2)\beta_i}{(1-\beta_s)^2} h_e, \tag{D6}$$

$$I_7 = n_i^2 \int d\vec{v} \frac{(1-\beta^2)\beta_i^2}{(1-\beta_s)^2} h_e, \tag{D7}$$

$$I_8 = (n_i^2 - 1) \int d\vec{v} \frac{(1-\beta^2)\beta_E^2}{(1-\beta_s)^2} h_e, \tag{D8}$$

$$I_9 = -(1-n_i c_\theta)^2 \int d\vec{v} \frac{(1-\beta^2)^2\beta_E^2}{(1-\beta_s)^4} h_e, \tag{D9}$$

where h_q is defined in Eq. (C2).

[1] J. Sheffield, *Plasma Scattering of Electromagnetic Radiation* (Academic Press, New York, 1975).
[2] S. H. Glenzer, C. A. Back, L. J. Suter, M. A. Blain, O. L. Landen, J. D. Lindl, B. J. MacGowan, G. F. Stone, R. E. Turner, and B. H. Wilde, Phys. Rev. Lett. **79**, 1277 (1997).
[3] D. H. Froula, L. Divol, and S. H. Glenzer, Phys. Rev. Lett. **88**, 105003 (2002).
[4] D. H. Froula, L. Divol, D. G. Braun, B. I. Cohen, G. Gregori, A. Mackinnon, E. A. Williams, S. H. Glenzer, H. A. Baldis, D. S. Montgomery, and R. P. Johnson, Phys. Plasmas **10**, 1846 (2003).
[5] N. Peacock, D. Robinson, M. Forrest, P. Wilcock, and V. Sannikov, Nature (London) **224**, 488 (1969).
[6] R. Behn, D. Dicken, J. Hackmann, S. Salito, M. Siegrist, P. Krug, I. Kjelberg, B. Duval, B. Joye, and A. Pochelon, Phys. Rev. Lett. **62**, 2833 (1989).
[7] F. Alladio and M. Martone, Phys. Lett. **60A**, 39 (1977).
[8] T. Wrubel, S. Buscher, and H. Kunze, Plasma Phys. Controlled Fusion **42**, 519 (2000).
[9] R. Pasqualotto, A. Sardella, A. Intravaia, and L. Marrelli, Rev. Sci. Instrum. **70**, 1416 (1999).
[10] J. D. Lindl *et al.*, Phys. Plasmas **11**, 339 (2004).
[11] W. L. Kruer, *The Physics of Laser Plasma Interactions* (Westview, Boulder, CO, 2003).
[12] R. Pechacek and A. Trivelpiece, Phys. Fluids **10**, 1688 (1967).
[13] H. Bindslev, Plasma Phys. Controlled Fusion **33**, 1775 (1991).
[14] M. Mattioli and R. Papoular, Plasma Phys. **17**, 165 (1975).
[15] J. S. Ross, S. H. Glenzer, J. P. Palastro, B. B. Pollock, D. Price, L. Divol, G. R. Tynan, and D. H. Froula, Phys. Rev. Lett. **104**, 105001 (2010).
[16] O. Naito, H. Yoshida, and T. Matoba, Phys. Fluids B **5**, 4256 (1993).
[17] T. Matoba, T. Itagaki, T. Yamauchi, and A. Funahashi, Jpn. J. Appl. Phys. **18**, 1127 (1979).
[18] K. V. Beausang and S. L. Prunty, Plasma Phys. Controlled Fusion **50**, 095001 (2008).
[19] N. A. Krall and A. W. Trivelpiece, *Principles of Plasma Physics* (San Francisco Press, San Francisco, CA, 1986).
[20] J. D. Jackson, *Classical Electromagnetism* (Wiley, New York, 1962).
[21] G. B. Arfken and H. J. Weber, *Mathematical Methods for Physicists* (Harcourt, New York, 2001).